ACCURACY STUDY OF A 450 KV CT SYSTEM WITH A CALIBRATED TEST OBJECT

Frank WELKENHUYZEN[1], Denis INDESTEEGE[1], Bart BOECKMANS[1], Kim KIEKENS[1,2], Ye TAN[1,2], Wim DEWULF[1,2] and Jean-Pierre KRUTH[1]

1 Katholic University Leuven, Celestijnenlaan 300B, 30001 Heverlee, Belgium, Frank.Welkenhuyzen@mech.kuleuven.be
2 Group T, KULeuven Association, A. Vesaliusstraat 13, 3000 Leuven, Belgium

Abstract

Computed tomography is already a well established technology in medical and material analysis. Also for dimensional metrology applications, CT is a promising technique for measuring internal and external geometries. Nowadays, most industrial CT scanners, use 120 to 225 kV sources. To scan thicker and more absorbing materials, more power is needed. The Nikon Metrology XT H450 has a range up to 450 kV. However the accuracy of these new, more powerful machines has to be investigated. This accuracy study uses a calibrated reference object and simulations, to get a better understanding of the existing errors. This reference object is developed and produced by fixing CMM probing styli on a socket. It has been produced in several materials and used together with simulations to analyze the accuracy of single and multi-material CT measurements. For single material, accuracies up to 10-15 µm are achieved. In the case of multi material this accuracy deteriorates to 70-80 µm. Besides some mechanical errors which cause these deviations, the main factor is the edge detection.

Keywords: Computed Tomography, Metrology, Simulation

1. INTRODUCTION

Computed Tomography (CT) is a well known technique in the medical world and in the field of material inspection. Its application field has recently been broadened to include dimensional metrology. CT enables measuring the objects' outside as well as its inside (e.g. invisible holes) in a non-destructive way. The ability to measure the inside of a part makes industrial Computed Tomography (Figure 1) attractive and unique in dimensional metrology. Assemblies, complex structures as well as the inner geometry of parts made by rapid manufacturing can be measured in a non-destructive way. This paper investigates the accuracy of a 450 kV CT scanner by means of a calibrated test object. Results obtained by CT measurements and simulations will be presented.

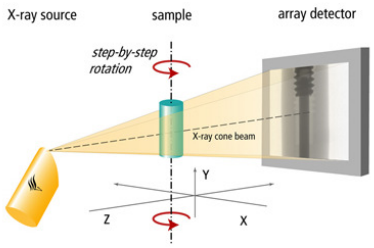

Fig. 1: Principle of industrial X-ray Computed Tomography (illustrated in case of a flat panel detector) [1].

2. HARDWARE AND SOFTWARE

2.1 Hardware

Nowadays, CT scanners for dimensional metrology purposes commonly reach a voltage of 225 kV. These scanners are built and fine tuned for such measurements. Special attention goes to the spotsize. The spotsize is defined as the spot where the electron beam hits the target to generate X-rays. A finite spotsize causes blurring at the edges of scanned object. For 225 kV CT scanners, nanofocus spots are available, which means that the spotsize is around or smaller than 1 µm. For larger objects or more absorbing materials, a higher power is necessary.

This is where the Nikon Metrology XT H450 comes into play. With a voltage up to 450 kV, the scanner is better equipped for penetrating thicker structures and materials with a high attenuation coefficient. But with these powers, the spotsize will be larger. The Nikon Metrology XT H450 has a minimum spotsize of 75 µm, which expands linearly with powers higher than 75 W. In combination with a conical beam, a 2D flat panel detector is used in the CT-scanner. The default settings comprise an exposure time of 1000 ms and 1000 projections. Settings of voltage and current will be chosen appropriately for each measurement.

2.2 Software: CTPro and VGStudio Max 2.2

After data acquisition, the 2D images are reconstructed using CTPro (reconstruction software of Nikon Metrology).

Ensuing volume reconstruction, the volume can be loaded in VGStudio Max 2.2 for further data processing and geometrical analysis. A critical step is edge detection or segmentation: determining the respective interfaces between solid materials and surrounding air or between different solid materials. The edge detection has been performed as follows in this paper: first a global threshold is determined by defining one threshold gray value. This results in a rough part contour. Hereafter the advanced surface determination of VGStudio MAX 2.2 is used: starting from the previous defined contour, a more accurate surface determination is obtained.

Further measurements have taken place in VGStudio.

2.3 Simulation program

A simulation program has been developed and is presented in earlier work [2]. By simulating CT scans, principles can be better understood and measurement errors can be related to different process parameters. Using the simulation program, 2D images are generated that can be

reconstructed into a 3D model like normal projections from a CT scan.

3. CALIBRATED OBJECT

3.1 Styli calibration object

To determine the accuracy of the 450 kV scanner used in this study, the necessity of reference objects arises. Today there is a lack of well defined reference objects and procedures suited to assess the accuracy of CT-based CMMs, and to compare the performance of various CT measuring devices [3]. Therefore a reference object is developed and produced by fixing CMM probing styli on a socket (figure 2 and figure 3), which has screw holes on distances 22.5, 37.5 and 52.5 mm to the center. The use of such styli has already been described in some literature [4]. The styli are made of ruby spheres on carbon fiber rods, with diameters 4, 6 and 8 mm. The application of the reference object is twofold. Firstly, it is possible to measure distances between sphere centers. Using sphere centers cancels out existing beam hardening and threshold errors. The sphere centers are independent of the sphere diameter. Secondly, sphere diameters can be measured to quantify beam hardening and/or threshold errors.

In a second step (section 4.4) new sphere materials have been introduced in the object. Figure 4 shows the extended stylus object and lists the materials.

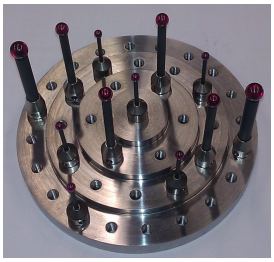

Fig. 2: Styli calibration object with ruby spheres only.

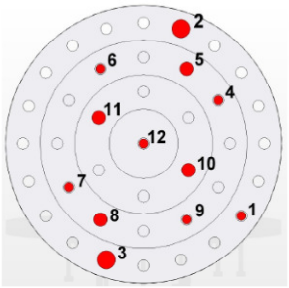

Distance	Sphere diameters
Dist. 2-3	8 mm
Dist. 10-11	6 mm
Dist. 5-8	6 mm
Dist. 4-7	4 mm
Dist. 6-9	4 mm
Dist. 4-12	4 mm
Dist. 6-12	4 mm
Dist. 7-12	4 mm
Dist. 9-12	4 mm

Fig. 3: Measured values: Schematic representation (left) and measured distances (right).

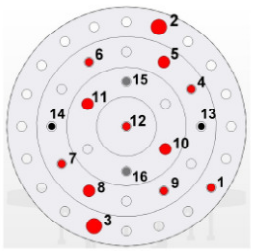

Material	Sphere #	Diameter
Al_2O_3	2,3	8 mm
	5,8,10,11	6 mm
	1,4,6,7,9,12	4 mm
Si_3N_4	13,14	3 mm
ZrO_2	15,16	4 mm

Fig. 4: Extended styli calibration object: Schematic representation (left) and sphere materials (right).

3.2 Calibration

As a reference, the sphere distances (listed in figure 3) between several spheres are measured with a conventional tactile CMM Mitutoyo FN 905 with specified accuracy: u1 = 4.2 + 5.L/1000 µm (with L in mm, for each axis). Each investigated distance has been measured 13 times, spread over 3 days. Afterwards the standard deviation on each distance has been calculated, resulting in a maximum standard deviation value of 1 µm. Figure 5 shows the CMM measurement results for the distance between spheres 2 and 3.

The specified nominal values have been used as reference values for the diameters, as the sphere diameters have sub micrometer accuracy.

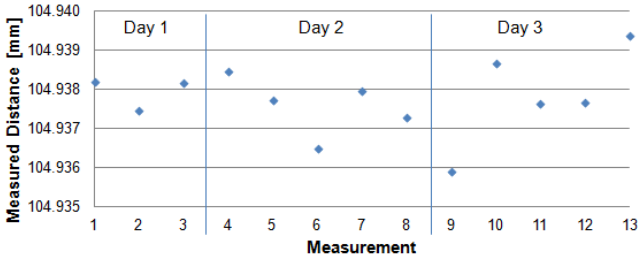

Fig. 5: Measured CMM distance (distance 2-3) in function of measurement number.

4. MEASUREMENT RESULTS

4.1 Distances

The investigated distances are listed and schematically represented in figure 3. CT measurements are repeated for different magnifications and filter plates (table 1).

After performing a CT scan and reconstructing the volume, this volume is loaded in VGStudio. Because of the inaccuracy of the magnification axis, it is necessary to rescale the volume. The volume can be rescaled by adjusting the voxelsize in VGStudio. Determining the correct voxelsize is done by compensating one of the CT measured distances to the "true" value (CMM measurement).

The volumes are rescaled two times: first on the smallest distance available (between spheres 10-11) and secondly on the largest distance (spheres 2-3). Figure 6 shows distance (dist.) 2-3, 10-11 and 6-9 in detail for the CT measurements made with a 2 mm Cu filter. It is evident from the numerical values and the graphs that rescaling on the largest distance (2-3) provides the best results: see distance between spheres 6-9 in figure 6 (distance between spheres 10-11 is obviously best when rescaling with distance 10-11). Although the results are better, errors of magnitude 10 µm still exist, with maximum deviations up to 15 µm. Notice also that with the settings used in figure 6 the most accurate measurements are obtained with the smallest magnification.

Table 1: Measurement setup: measurements (left) and used settings per filter (right).

	Magn. [/]	Voxelsize [mm]
Meas. 1	2.66	0.075
Meas. 2	2.21	0.091
Meas. 3	1.88	0.106
Meas. 4	1.64	0.122
Meas. 5	1.46	0.137

Filter	Voltage [kV]	Current [µA]
2 mm Cu	200	270
No filter	125	133
3 mm Al	135	145

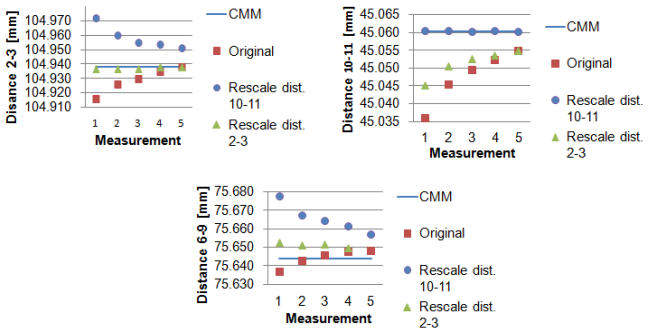

Fig. 6: Resulting distance in function of measurement for distance 2-3 (top left), 10-11 (top right) and 6-9 (bottom).

4.2 Diameters

Considering the sphere diameters, rescaling has no effect. Figure 7, left, presents the 4 mm sphere diameters after rescaling on distance 2-3. The large deviations shown have two causes. First of all, the transition between the ruby sphere and the carbon fiber rod introduces imperfections at the location where the sphere surface is interrupted to provide room for the carbon rod. This imperfection will induce errors in the algorithm that defines the spheres, causing incorrect results. Secondly, despite the use of VGStudio's advanced mode edge detection, the final contour is highly dependent of the starting contour. Both problems can be largely solved by using a region of interest (ROI). When selecting as ROI the region only containing the sphere is used, the transition part between ruby and carbon is eliminated. Figure 7, right, shows the improved results. This however gives no enhancement for the measured distances.

When observing figure 7 there seems to be a trend for all measurements: the diameter of the center sphere (sphere 12, that is located on the rotation axis of the CT scanner while measuring) is always the largest, the sphere the furthest away from the center (sphere 1) always has the smallest diameter and the other spheres seem to have comparable diameters. As a test, a new CT scan has been executed with sphere 6 closest to the rotation axis. The results are shown in figure 8. A similar trend is present. Again the sphere diameters are dependent of the distance to the axis of rotation. Figure 9 shows the fit points of two spheres: the sphere near the axis of rotation and another sphere. It is clear that the latter sphere suffers from a form deviation. This observation will be further investigated using simulations in section 4.4.

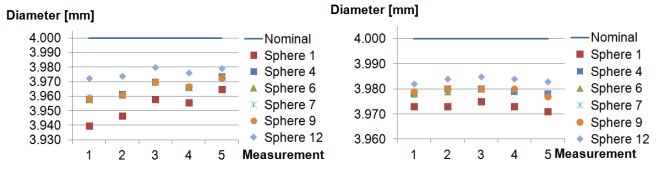

Fig. 7: Measured sphere diameters: when rescaling on distance 2-3 (left) and after selection of ROI (right). (The markers of spheres 4, 6, 7 and 9 are laying on top of each other and therefore not separately visible.)

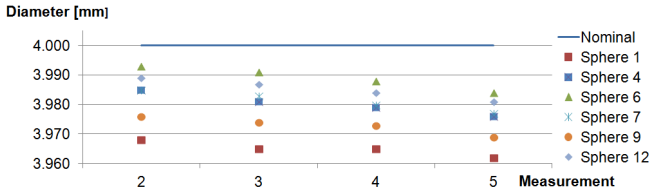

Fig. 8: Measured sphere diameters in case of sphere 6 near the axis of rotation. (Only measurements 2 to 5 have been executed).

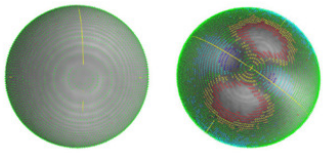

Fig. 9: Fitpoint deviations: Sphere near the rotation axis (left) and other sphere (right).

4.3 Filter plates

Using a filter plate, like 2 mm copper from previous measurements, gives the advantage that it absorbs the soft X-rays. Absorbing these low energy X-rays in the filter, avoids beam hardening in the object. But with a thicker filter, a higher power setting is necessary as shown by the settings in table 1. This higher power level can decrease the signal-to-noise ratio, which deteriorates the results.

However, comparing the results of the 2 mm copper, the 3 mm aluminum and when using no filter shows no significant differences for the presented measurements.

4.4 Extended styli object

A 3 mm aluminum filter is used in combination with 150 kV and 130 µA to measure a combination of ruby (Al_2O_3), silicon nitride (Si_3N_4) and zirconium oxide (ZrO_2) spheres. The same measurements are performed in accordance with table 1.

The major differences with the full ruby equivalent are situated in the sphere diameters. Figure 10 presents the 4 mm diameter spheres for the measurements. Large errors are visible for the ZrO_2 spheres (sphere 15 and 16), even when ROI's are created. These large deviations are probably introduced in the edge detection algorithm. ZrO_2 has a higher attenuation coefficient, so the gray values for these spheres differ a lot from the gray values of the ruby and Si_3N_4 spheres.

Regarding the distances between sphere centers the results equal previous results from section 4.1.

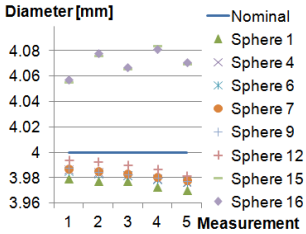

Fig. 10: Measured sphere diameters of extended styli object. (The markers of spheres 4, 6, 7 and 9 are laying on top of each other and therefore not separately visible. The same is true for the markers of sphere 15 and 16.)

4.5 Simulations

As already discussed in section 4.2 there seems to be a relationship between the sphere diameters and the distance to the axis of rotation (of the rotation table). Alignment errors (the rotation axis is supposed to be aligned parallel, resp. perpendicular to the detector and its pixel rows or columns [3]) can be one of the reasons of this trend. Simulations have been executed to investigate this. The results of two simulations will be presented here. Without going into detail, table 2 shows the simulation parameters (axes directions as defined in figure 1). One simulation contains several errors: Translation (shift) and rotation (tilt) of the rotation axis and detector, eccentricity of the rotation table, tangential source drift… have been implemented. The values for the errors are obtained by investigation (using a laser interferometer and electronic levels) and/or are found in literature. The other simulation represents the ideal case (without errors).

Figure 11 shows the fitpoints of the sphere closest to the axis of rotation and another sphere when there are no alignment errors implemented and when there are alignment errors implemented. It is clear that the fitpoint deviations are similar to these of the real measurements (see figure 9) in case of the simulation with errors. In case of the simulation without alignment errors, all spheres have similar fitpoint deviations. Figure 12 shows the calculated diameters for the 4 mm sphere diameters in case of the simulation with errors (sphere 12 on the rotation axis and magnification 2.66). A similar trend can be seen as for the real CT measurements (see figure 7). In case of the simulation without errors, this trend was not there.

Table 2: Simulation parameters.

Parameter	with errors	without errors
Voltage	200 kV	200 kV
Current	270 µA	270 µA
Filter plate	2 mm Cu	2 mm Cu
Spotsize	80 µm	80 µm
Source drift	tan 20 µm	0
Distance Source Object	386.46 mm	386.46 mm
Number of Rotation Steps	1001	1001
Rotation axis shift in x direction	0.04 mm	0
Rotation axis shift in z direction	0.04 mm	0
Tilt rotation axis around z	0	0
Tilt rotation axis around x	5/1000	0
Rotation axis overshoot	0.042°	0
Wobble	0	0
Eccentricity	0.002 mm	0
Tilt detector around z	0	0
Tilt detector around x	-3/1000	0
Tilt detector around y	-1.5/1000	0
Shift detector in x direction	-0.65 mm	0
Shift detector in y direction	-0.8 mm	0

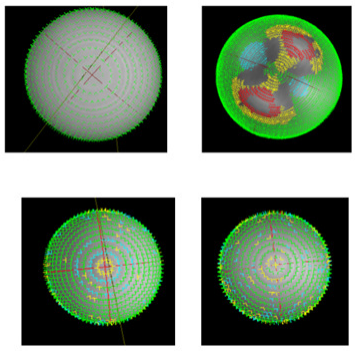

Fig. 11: Fitpoint deviations: Sphere near the rotation axis (left) and other sphere (right) for simulation with errors (top) and the ideal case (bottom).

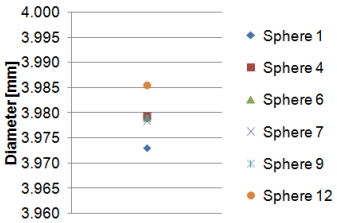

Fig. 12: Measured sphere diameters of the simulation containing several (alignment) errors. (The markers of spheres 4, 6, 7 and 9 are laying on top of each other and therefore not separately visible.)

5. CONCLUSIONS

The accuracy between sphere centers is approximately 10-15 µm, mostly independent on the filter and settings used. Sphere diameters experience a threshold error. Therefore results will depend on threshold choice. This dependency can be reduced by using a region of interest. For a single material object, the sphere diameters have an accuracy up to 20-30 µm. In multi-material measurements, this accuracy deteriorates sharply to 70-80 µm for the materials with higher attenuation coefficients.

Simulations show that those inaccuracies can be introduced by, among others, shift of the detector screen and tilt of the rotation axis. A simulation with errors similar to the real CT scanner gave similar measurement results.

REFERENCES

[1] Phoenix X-ray, http://www.phoenix-xray.com.

[2] F. Welkenhuyzen, B. Boeckmans, J.P. Kruth, W. Dewulf, A. Voet, Simulation of X-ray projection images for dimensional CT metrology, 2012, proceedings of the 5th international conference on optical measurement techniques for structures and systems pages:477-487.

[3] J.P. Kruth, M. Bartscher, S. Carmignato, R. Schmitt, L. De Chiffre, A. Weckenmann, 2011, Computed Tomography for Dimensional Metrology, CIRP Annals - Manufacturing Technology, 60/2:821-842.

[4] H. Lettenbauer, B. Georgi, and D. Weiß. Means to verify the accuracy of ct systems for metrology applications (in the absence of established international standards). DIR - International symposium on digital industrial radiology and computed tomography, 4, 6 2007.